Ultrasound in Med. & Biol. Vol. 16, No. 6, pp. 561–569, 1990
Printed in the U.S.A.

0301-5629/90 $3.00 + .00
© 1990 Pergamon Press plc

●*Original Contribution*

QUANTITATIVE TISSUE MOTION ANALYSIS OF DIGITIZED M-MODE IMAGES: GESTATIONAL DIFFERENCES OF FETAL LUNG†

RONALD S. ADLER, JONATHAN M. RUBIN, PEYTON H. BLAND and PAUL L. CARSON
Department of Radiology, University of Michigan, Ann Arbor, MI 48109

(*Received* 3 *November* 1989; *in final form* 26 *March* 1990)

Abstract—Quantitative analysis of transmitted cardiac motion in fetal lung is evaluated by applying correlation techniques to digitized M-mode images in 21 patients, subdivided into two subgroups by gestational age: (I) 25–30 weeks (11 patients), and (II) ≥35 weeks (10 patients). The corresponding numbers of M-mode images analyzed for each group are 23 and 18, respectively. This partition is expected to reflect functionally "immature" and "mature" lungs. The estimated maximum mean radial deformation per unit epicardial excursion, $\langle r \rangle$, is calculated from the two-time, spatially averaged correlation function obtained between diastolic and systolic M-mode lines. The collective results for each subgroup are $\langle r \rangle$ I = 0.79 ± 0.11 (sem) and $\langle r \rangle$ II = 0.62 ± 0.13 (sem). The analysis presented, albeit in a limited population, is indicative of a trend in accordance with qualitative observations of Birnholz and Farrell (1985). M-mode analysis, as indicated by Adler et al. (1989) is a potentially useful technique to quantify such tissue motion.

Key Words: **Digitized M-mode, Fetal lung, Tissue motion.**

INTRODUCTION

The noninvasive assessment of fetal growth and development is a routinely performed examination. This entails measurement of sonographically determined growth parameters which relate to mean gestational age, fetal well-being, as well as the qualitative evaluation of the fetus and its environment (Callen 1983). Tissue characterization may provide additional important information regarding fetal development. While the latter has been primarily qualitative in nature, for example, the relative liver/lung echotexture as an indicator of fetal pulmonary maturity, extensive efforts have been directed toward quantifying these subjective features in terms of measurable physical parameters (*e.g.*, linear attenuation coefficient) (Adler et al. 1989; Thieme et al. 1983; Carson et al. 1986, 1989; Birnholz and Farrell 1985).

Recent work by Birnholz and Farrell (1985) suggests that transmitted cardiac motion in fetal lung may similarly reflect pulmonary maturity, although their results are, perhaps, overly optimistic. That such a relationship exists would not be entirely surprising in as much as tissue motion relates directly to mechanical properties such as shear elastic modulus (Adler et al. 1989). While qualitative analysis of transmitted cardiac motion is of some value, a quantitative approach may ultimately be more useful for several reasons:

1. It will provide a mechanism to definitively establish whether a relationship between lung elasticity and pulmonary maturity does, in fact, exist.
2. Relevant variables, both intrinsic (*e.g.*, shear elastic modulus) and extrinsic (*e.g.*, rate of deformation), may be identified.
3. Comparison to other well-established indicators of pulmonary maturity, such as lecithin/sphingomyelin (L/S) ratio, is facilitated.
4. The presence of an appropriate "lung elasticity" parameter enables assessment of interval changes with increasing gestational age, thereby aiding in clinical management of the fetus at risk for early delivery.

In recent years, tissue motion analysis has provided insight into normal tissue viscoelastic properties, as well as differentiating normal and pathologic tissue (Birnholz and Farrell 1985; Meunier et al. 1988; Adler et al. 1989; Tristam et al. 1986, 1988; Truong et al. 1978; Krousop et al. 1987; Lerner et al.

† This work was supported in part by PHS Grant No. R01HD17243 awarded by the National Institute for Human Growth and Development (DDHS).

1988). Within the context of the current work, the radial deformation of fetal lung by adjacent cardiac activity is followed by M-mode scans obtained at the time of obstetrical ultrasound. As indicated by Adler et al. (1989), M-mode images contain information regarding the deformation profile as a function of distance from the epicardial surface, by tracking the motion of specular reflectors which persist throughout the cardiac cycle. A parameter which serves to characterize the range of transmitted cardiac motion in fetal lung is demonstrated to be the time and spatially averaged systolic to diastolic deformation per unit epicardial displacement, $\langle r \rangle$ as this may be readily accessible to routine obstetrical ultrasound examination.

In the current work, correlation techniques are applied to digitized M-mode images in two trial clinical subgroups of women undergoing obstetrical ultrasound: those that exhibit a strong predominance of immaturity or maturity by their gestational ages, 25–30 weeks or greater than 35 weeks, respectively (Gluck et al. 1974). The former represents a potential risk group for development of hyaline membrane disease following premature delivery. It is demonstrated that these techniques can provide an estimate for $\langle r \rangle$, which, for the limited population considered, suggests a trend in accordance with the qualitative observations of Birnholz and Farrell (1985).

A description of this approach is first considered along with simulation data in the absence of noise for purposes of illustration. The latter provides insight into the use of correlation techniques to track motion of specular reflectors within fetal lung. Examples are presented in the case of two and three specular reflectors. An approximate expression to calculate mean lung deformation resulting from adjacent cardiac motion is derived. Since actual gray-scale data will exhibit variable peak heights, a simple scaling procedure is implemented, which does not alter peak location or morphology, in order to apply this expression, eqn (2), to estimate mean lung deformation.

THEORY AND SIMULATION

In order to establish the applicability of correlation analysis in evaluating tissue motion, simulation examples will be presented. Because of spatial smoothing, correlation functions are well suited to examine tissue displacements in the presence of noisy data (Oppenheim and Schafer 1989; Papoulis 1965). For purposes of illustration, we first consider simulated gray-scale peaks undergoing differential translation in the absence of noise. The importance of following both position and amplitude information in the resulting correlation functions is illustrated.

Typical time-averaged M-mode data will consist of a series of peaks distributed along a line bounded by fetal epicardium and chest wall (~2 cm in dimension) in which the mean gray scale intensity (*i.e.*, background) has been subtracted. This latter step simplifies subsequent correlation analysis. Two such gray-scale distributions are considered corresponding to systole and diastole. Time averaging is performed over multiple (usually 3–6) cardiac cycles. As indicated by Adler et al. (1989) M-mode data (Fig. 4) displays well-defined motion of specular reflectors distributed throughout the fetal lung. The resulting gray-scale distributions (Fig. 5) will display multiple peaks distributed along a given M-mode line. Idealized gray-scale data for two specular reflectors is depicted in Fig. 1 for slight "lung" deformation. In simulated raw data, the peak situated most closely to the origin (Fig. 1) reflects epicardial motion, while the remaining peak represents corresponding lung parenchymal excursion. Correlation data for two and three simulated specular peaks (noiseless data) is presented in Fig. 2 (see discussion below).

Mathematical treatment in the case of an arbitrary number of specular reflectors is presented in the Appendix. Let $f_s(x)$ and $f_d(x)$ denote the subtracted time-averaged gray-scale distributions for systole and diastole, respectively. Cross-correlation of this data is performed by the prescription

$$\Phi_{sd}(y) \equiv \int f_s(x) f_d(x + y) dx, \qquad (1)$$

producing a function of the shift parameter y in which the integration is performed over the epicardial/chest wall distance. In the case for which f_s and f_d are related by pure translation (Fig. 2a), $\Phi_{sd}(y)$ displays multiple peaks, the largest of which occurs at about 19 pixels corresponding to the amount of translation, the latter being designated as the primary peak or, equivalently, primary peak complex in the ensuing discussion. Displacement of distal reflectors somewhat less than the epicardium results in either slight shift and broadening or splitting of this primary peak, depending upon the differential translation between specular peaks. This is evident in the case of a 5-pixel relative displacement (Fig. 2b) in which there is slight broadening and shift of the primary correlation peak, while a 10-pixel deformation (Fig. 2c) which exceeds the full width at half maximum (FWHM) of the simulated peak results in splitting. Furthermore, this shift or splitting is directed toward values of y less than the epicardial excursion.

When three specular reflectors are present, in addition to primary peak splitting or broadening, the relative amplitude of subpeaks must be accounted for

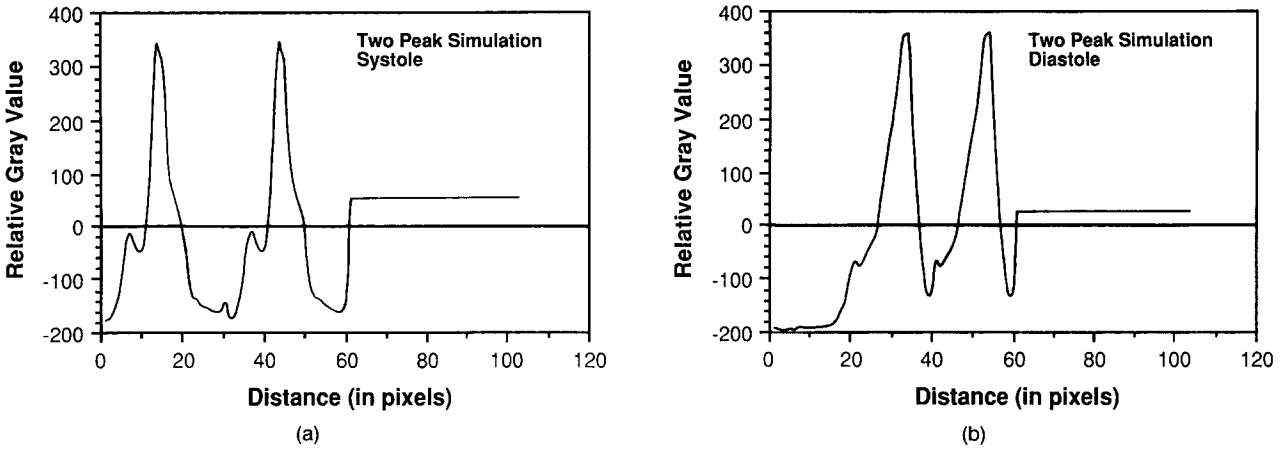

Fig. 1. Simulated gray-scale data for two specular reflectors following time-averaging and subtraction of mean gray-scale intensity. Ordinate axis denotes relative gray-scale intensity (arbitrary units) versus distance in pixels (arbitrary units). The peak closest to the origin represents the epicardial reflector with the more distal peak denoting the "parenchymal" specular reflector. Curves (a) and (b) denote systolic and diastolic data, respectively. There is a 10-pixel differential translation between the first and second peak in diastole simulating lung elasticity. Varying degrees of elastic response are introduced by adjusting the amount of differential motion of the second peak. Similarly, multiple peaks undergoing variable amounts of translation can be considered.

as indicated in the Appendix. For example, suppose that two parenchymal peaks are displaced equally, but less than the epicardium (Fig. 2d), the primary peak then consists of a couplet with the proximal component being approximately a factor of two greater in amplitude than the distal component.

In view of these considerations, mean radial deformation per unit epicardial displacement, $\langle r \rangle$, may be estimated according to eqns (A4–6),

$$\langle r \rangle \approx \sum_{j=1}^{N_P} \Phi_j \Delta_j / \sum_{j=1}^{N_P} \Phi_j \Delta_E, \tag{2}$$

in which Δ_j and Φ_j refer to location and amplitude of the jth component of the primary correlation peak, $j = 1, 2, \ldots, N_P$, respectively, the sum being performed over all components of the primary peak, and $\Delta_E = \Delta_{N_P}$ refers to the epicardial displacement. Δ_E can be directly estimated from the gray-scale data or by performing local cross-correlation in that part of the M-mode image limited to the epicardium. The component peaks occurring at locations $\{\Delta_j\}_{j=1}^{N_P}$ are defined as those peaks in the cross-correlation plot for which $\Delta_j \leq \Delta_E$. Since no reflector, in our experience, is displaced by an amount greater than the epicardium, this prescription is at least empirically justified.

The accuracy of such an estimate is clearly limited by sampling of only relatively few points. In view of the observed slow monotonic decrease in the deformation profile, such an estimate is expected to yield reasonable results for an adequate number of specular reflectors (probably ~3–4) distributed relatively uniformly throughout the fetal lung. The problems posed by amplitude variation in real data are dealt with in a subsequent section.

MATERIALS AND METHODS

All examinations were performed with informed consent of the mothers, under protocols approved by the institutional review board. The study group consisted of pregnant volunteers and patients undergoing routine obstetrical ultrasound examination. Gestational age estimates were based on conventional growth parameters (biparietal diameter, femur length, abdominal circumference), accurately known menstrual history and prior ultrasound measurements when available. All patients examined had no known predisposing factors which would unfavorably affect fetal well-being (*e.g.*, hypertension, smoking, diabetes melitus, etc.). Two gestational subgroups were selected which are expected to fairly reliably separate the pulmonary immature (25–30 weeks) and pulmonary mature fetuses (≥35 weeks). Fetal outcome data was available in 13/21 patients who delivered at term with no significant fetal abnormality in the immediate post-natal period.

Images were obtained using 3.5 and 5 MHz variable focused phased array scanners in either sector or linear mode (General Electric 3600, Radius, Milwaukee, WI) and in either combined B/M-mode or M-mode display. The anatomic plane of imaging, as described by Adler et al. (1989), is transverse through the fetal thorax with radial lines of data taken through

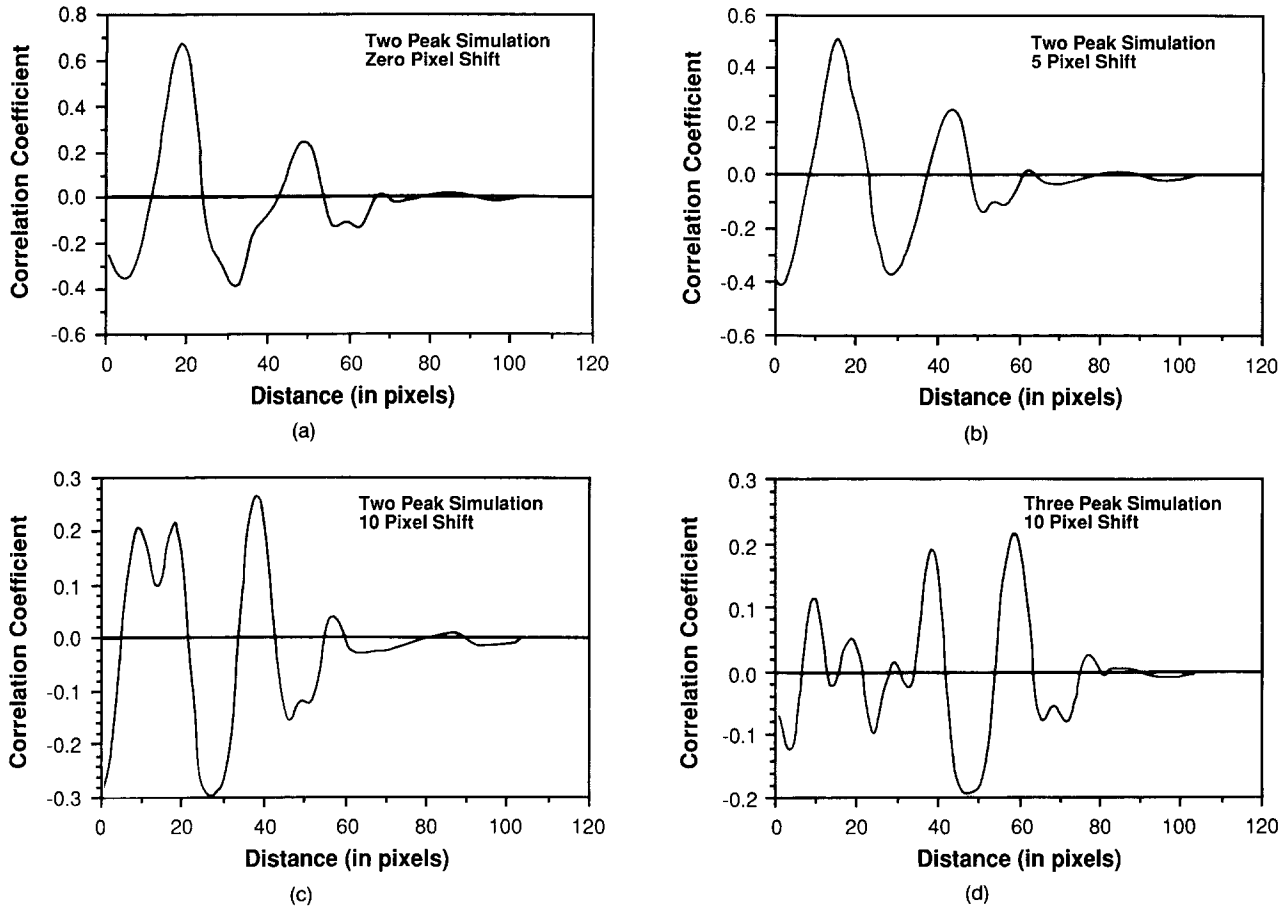

Fig. 2. Correlation coefficient obtained from simulated systolic and diastolic gray-scale data. (a) Correlation data for two specular peaks undergoing equal translation. Notice that the primary peak occurring at about 19 pixels corresponds to the net epicardial excursion in going from systole to diastole in Fig. 1. (b) Correlation data for two specular peaks undergoing mild differential translation (5 pixels). The primary peak is slightly broadened and shifted toward the origin. (c) Correlation data for two specular peaks undergoes a 10-pixel differential motion (Fig. 1). The primary peak complex forms a couplet separated by 10 pixels. (d) Correlation data for three specular reflectors in which two "parenchymal" peaks translate equivalent amounts. The corresponding gray-scale distribution (not shown) is arrived at by placing a third peak in Fig. 1a at ~75 pixel location. In the resulting diastole, each of the parenchymal peaks is shifted by an amount 10 pixels less than the epicardium. The primary peak is then a couplet in which the proximal component is a factor of two greater in amplitude, than the distal component.

the left ventricle and perpendicular to the interventricular septum (Fig. 3). At this level the adjacent lung deformation by fetal cardiac motion is maximal. M-mode images were then digitized to 512 × 512 matrix using a VICOM 1850 digital image processing system (VICOM Systems Inc., San Jose, CA) with approximately 7-bit dynamic range in the analog to digital conversion.

Only images that displayed well-defined motion of individual specular reflectors distributed throughout the fetal lung and over several systolic/diastolic couplets were selected to digitize. Since this latter feature was not a requirement in acquiring images, no attempt is made to estimate our success in obtaining such data.

A rectangular Region of Interest (ROI) extending from the epicardium up to, but not including, the fetal chest wall was interactively selected. Radial lines of data corresponding to extremal positions of the epicardium and a horizontal line to denote approximate range of epicardial motion were chosen from data within the ROI (Fig. 4). The fetal chest wall is recognized as a fixed bright specular peak easily identified in the M-mode image.

Digital image processing was performed utilizing a VAX 11/750 (Digital Equipment Corporation, Maynard, MA) and Mercury array processor (Mercury Computer Systems, Lowell, MA). The VICOM 1850 was interfaced with the VAX. Time averaging of systolic/diastolic couplets over multiple cardiac

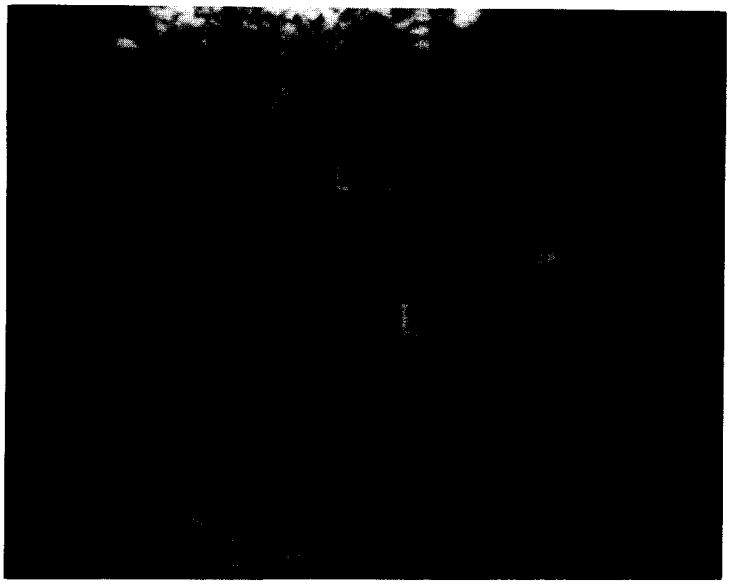

Fig. 3. Transverse image through the fetal thorax obtained in sector mode at the anatomic level used for M-mode acquisition. Radial lines of data, roughly perpendicular to the interventricular septum, are obtained including fetal epicardium (E) extending to fetal chest wall (CW). L denotes fetal lung.

cycles within the ROI and subsequent subtraction of mean gray-scale intensity enables approximate removal of the effects of random scatterers (*i.e.*, speckle). The resulting gray-scale distribution obtained from a 37-week gestation is illustrated in Fig. 5. Multiple, well-defined peaks occur at the mean

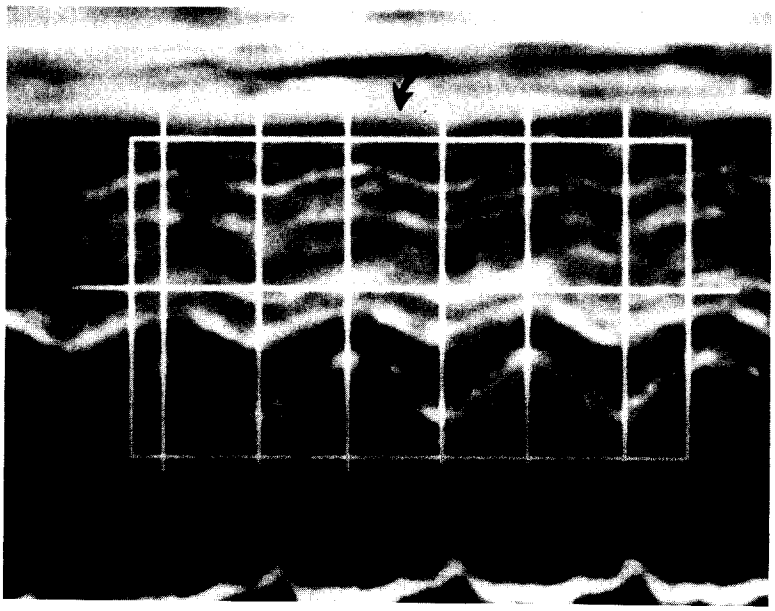

Fig. 4. M-mode record from a 37-week gestation with superimposed region-of-interest (ROI) used for M-mode analysis. Ventricular wall motion (open arrow) is seen as a distinct broad specular reflector surrounded on either side by fluid with adjacent fetal lung undergoing deformation. Well-defined specular reflectors (straight solid arrow) undergoing motion are distributed relatively uniformly throughout the fetal lung. A prominent fixed bright echo (curved solid arrow) immediately adjacent to fetal lung denotes fetal chest wall. The ROI includes the ventricular/epicardial peak, which demonstrates the greatest differential motion, and adjacent lung up to, but not including, the chest wall. Radial lines of data from 3 diastolic/systolic couplets were interactively selected. The horizontal line approximately separates transmitted lung data from ventricular wall/lung surface motion. This partition is utilized to obtain scaling coefficients for subsequent correlation analysis. The epicardial/chest wall distance in this example is ~2 cm with an epicardial excursion of ~4 mm in going from systole to diastole.

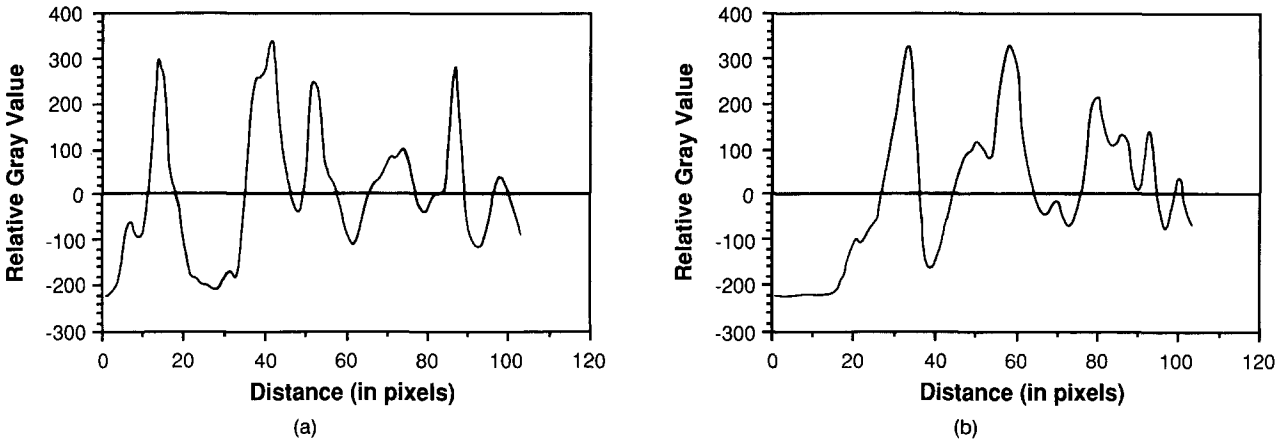

Fig. 5. Example of the time-averaged relative gray-scale distribution obtained from (a) systolic and (b) diastolic lines of data in the 37-week gestation presented in Fig. 4. Multiple peaks corresponding to bright reflectors in the M-mode image are distributed relatively uniformly throughout the fetal lung. Approximate distance conversion in this example is ~0.22 mm/pixel. The epicardial reflector results in the peak closest to the origin, which subsequently undergoes the maximum shift in going from systole to diastole relative to the remaining gray-scale peaks.

locations of specular reflectors in the M-mode image. In as much as the final estimate of lung deformation is expressed as a ratio, the abscissa is expressed in terms of arbitrary units (pixels).

Epicardial/chest wall distances of ~2 cm with maximum epicardial excursions of ~4–5 mm are typical. Displacements ~mm are easily resolved using this technique. ROI's were somewhat variable with lines of data represented by ~75–100 pixels corresponding to conversion factors of ~0.2–0.27 mm/pixel.

Motion analysis requires specular reflectors both proximally and distally in fetal lung, relative to the epicardium. We, therefore, require the presence of at least one peak at greater than 50% of the epicardial–chest wall distance. The epicardial reflector provides an estimate of immediately adjacent lung tissue motion. Gray-scale peaks were defined as those positive deflections whose subtracted gray value is greater than or equal to zero. This choice appears to correspond well with the location of specular reflectors in the corresponding M-mode image.

Application of eqn (2) to estimate mean lung deformation requires that specular peaks be of comparable amplitude. However, as is evident in Fig. 5, the epicardial peak is generally larger than the remaining specular peaks, in several cases by as much as a factor of 2. To partially compensate for this discrepancy, a simple scaling procedure is introduced whereby the mean power spectral density due to peaks distal to the horizontal line in the ROI is scaled to be equivalent to the epicardial contribution. Correlation analysis of resulting rescaled diastolic and systolic data was then performed for individual M-mode records satisfying the above criteria. Mean lung deformation was calculated from the resulting cross-correlation data employing eqns (A4–5). Epicardial excursion was estimated either directly from the raw data or by performing cross-correlation of epicardial data (points proximal to the horizontal bar in the ROI) and observing the location of the primary correlation peak.

RESULTS AND DISCUSSION

Birnholz and Farrell (1985) regard mature lung as easily deformed by adjacent cardiac motion, whereas immature lung, being less compliant, tends to move *en bloc*. They have applied a dynamic scoring system to evaluate tissue motion during real-time examination to distinguish "compliant, stiff and intermediate" patterns of lung motion. Let us consider their results assuming stiff and intermediate patterns correspond to immaturity, while a compliant pattern corresponds to maturity. Based on outcome data in 54 fetuses scanned within 36 h of delivery, the sensitivity and specificity for predicting lung immaturity derived from their data are 100% and 84%, respectively. Data for 60 fetuses < 29 weeks (immature) and 51 fetuses ≥ 37 weeks (mature) EGA suggest sensitivity and specificity of 87% and 80%, respectively.

This qualitative analysis suggests the potential utility of assessing transmitted cardiac motion in fetal lung as an indicator of pulmonary maturity. The ability to successfully apply such an observation to evaluate changes in lung elasticity with increasing gestational age requires a quantitative measure which ideally would be easily determined at the time of

obstetrical ultrasound. M-mode analysis, as indicated by our simulation results and the clinical example presented herein, does in fact, display such transmitted motion in a quantifiable fashion. Our results, however, are not so optimistic as previous qualitative analysis would indicate.

Simulations presented in the case of two and three specular reflectors indicate that the effect of lung motion is either to shift and broaden the primary correlation peak or to cause splitting of the primary peak. Both location and amplitude information of individual components are used to estimate mean parenchymal deformation (eqn 2). The cross-correlation coefficient for the same 37-week gestation presented in Figs. 4–5 is illustrated in Fig. 6. The epicardial displacement, estimated from the raw data, occurs at approximately 19 pixels. The estimated mean parenchymal deformation per unit epicardial displacement $\langle r \rangle$ for this example is ~0.63.

Evaluation of the remaining patient data which satisfy the requirement for digital analysis results in a scatter plot for the two gestational subgroups considered herein (Fig. 7). This particular division separates a group, commonly an at-risk group for Hyaline membrane disease, following premature delivery, from that pregnancy group which is typically considered to be at or near term.

If we further consider the set of points within each subgroup as constituting independent measurements for two presumed states of fetal pulmonary maturity, we obtain mean ratios as follows:

$$\langle r \rangle_{\mathrm{I}} = 0.79 \pm 0.11 \text{ (sem)},$$

$$\langle r \rangle_{\mathrm{II}} = 0.62 \pm 0.13 \text{ (sem)},$$

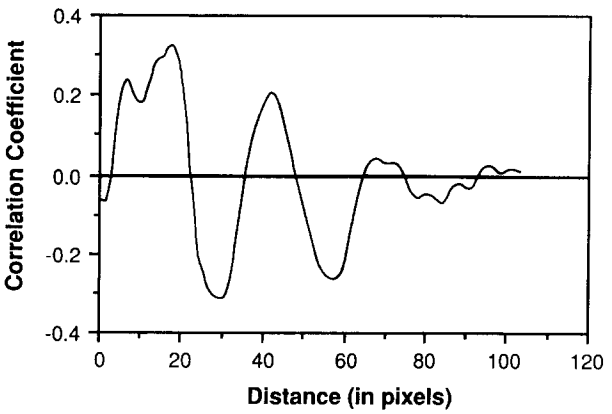

Fig. 6. Correlation coefficient obtained from a 37-week gestation (Fig. 4). The primary peak complex is a couplet with differing amplitude components. Estimated epicardial excursion from the raw data was 19 pixels (~4 mm) resulting in mean parenchymal deformation per unit epicardial displacement of ~0.63 following application of eqn (2).

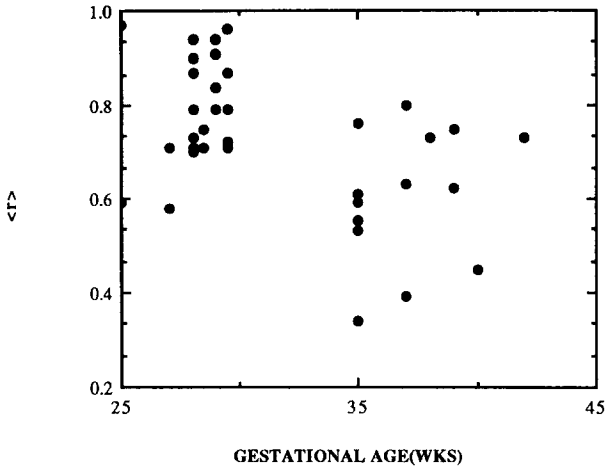

Fig. 7. Scatter plot of estimated mean lung deformation ratio per unit epicardial excursion (ordinate axis), $\langle r \rangle$, as a function of gestational age (abscissa) for the two gestational subgroups (25–30 weeks, ≥35 weeks) considered herein. A trend towards smaller values of $\langle r \rangle$, corresponding to greater lung deformation, is apparent with increasing gestational age.

where I (11 patients, 23 M-modes) and II (10 patients, 18 M-modes) refer to early (25–30 weeks) and late (≥35 weeks) gestational ages, respectively. Alternatively, comparison of the mean radial deformation ratios, r, in which the mean ratios for individual patients are first calculated, and compared to remaining patient data results in

$$r_{\mathrm{I}} = 0.76 \pm 0.11 \text{ (sem)},$$

$$r_{\mathrm{II}} = 0.62 \pm 0.1 \text{ (sem)},$$

with associated mean standard deviations, σ, for individual patients given by

$$\sigma_{\mathrm{I}} = 0.1,$$

$$\sigma_{\mathrm{II}} = 0.08,$$

which is comparable to the variation between patients. In either situation, utilizing Student's t-distribution, or nonparametric tests of significance, these values do not definitively differentiate functionally mature and immature lung ($p > .05$) (Colton 1974). These results do, however, indicate a trend suggesting the validity of Birnholz and Farrell's (1985) observations.

The data presented suggest that differences in lung elasticity *may* separate the pulmonary mature and immature fetuses indicating the necessity to further refine tissue motion analysis techniques, thereby improving estimates of the deformation ratio $\langle r \rangle$. Further clinical validation would require larger popu-

lations and/or longitudinal studies of individual patients with attention to technique in obtaining appropriate images for digital analysis.

No attempt has been made to adjust the data for variation in fetal cardiac rate. As indicated by Adler et al. (1989), the estimated degree of lung motion should vary with the rate of surface deformation (*e.g.*, heart rate), although such effects are expected to be ~5–10%, probably comparable to measurement error. The effect of varying rates of deformation will be investigated for an *in-vitro* model of tissue compression in a future work.

Sampling of individual specular reflectors within a given M-mode image provides a relatively sparse data set to estimate tissue motion, although, as indicated earlier, this may be sufficient in the present case for which the deformation profile appears to be a slowly varying function. Increasing the number of measurements for a given patient should improve the estimated mean deformation ratio, $\langle r \rangle$, assuming that fetal lung is indeed isotropic. A potential technique to improve upon current limitations presented by sparse data is to take full advantage of the three-dimensional data set by observing correlated motion in two and/or three dimensions. Furthermore, finer sampling achievable by observing patterns of speckle motion rather than specular reflectors may ultimately provide the best estimate of local tissue deformation (Meunier et al. 1988).

SUMMARY

Correlation techniques have been applied to M-mode data in order to quantitate local fetal lung deformation by adjacent cardiac activity. In particular, cross-correlation of the relative gray-scale data obtained from digitized M-mode scans averaged over multiple cardiac cycles taken with eqn (2) provides an estimate of the spatially averaged radial deformation of fetal lung in going from systole to diastole. Time averaging approximately removes effects of random scatterers so that only specular reflectors are considered. Amplitude variation in the specular peaks is accounted for on the average by virtue of scaling parenchymal data prior to performance of cross-correlation. No additional signal processing has been applied to the data. Observation of both location and amplitude of the primary peak multiplets in the correlation coefficient then allows estimation of the mean radial deformation per unit epicardial displacement, $\langle r \rangle$, provided that well-defined specular reflectors are distributed throughout the lung.

Quantitative results in a limited population indicate that a relationship between fetal lung elasticity and pulmonary maturity probably exists, although lung elasticity may not be sufficiently sensitive to distinguish the pulmonary mature and immature fetus. Alternatively, definitive clinical trials will require a large patient population and/or longitudinal studies of individual patients. Direct measurement of lung deformation as a function of alveolar surface tension in an appropriate animal model would establish the absolute validity of such a relationship. Further refinement in tissue motion quantification as well as better utilization of available gray-scale data should improve estimates of local tissue deformation.

Acknowledgments—The authors would like to express their appreciation to Teresa Wischer for secretarial assistance in preparation of the manuscript.

REFERENCES

Adler, R. S.; Rubin, J. M.; Bland, P. H.; Carson, P. L. Characterization of transmitted motion in fetal lung: Quantitative analysis. Med. Phys. 16(3):333–337; 1989.

Birnholz, J. C.; Farrell, E. E. Fetal lung development: Compressibility as a measurement of maturity. Radiology 157:495–498; 1985.

Callen, P. W. Ultrasonography in obstetrics and gynecology. Philadelphia, PA: Saunders; 1983.

Carson, P. L.; Meyer, C. R.; Bowerman, R. A.; Bland, P. H.; Bookstein, F. L. Prediction of pulmonary maturity from ultrasound scattering. In: Greanleaf, J. F., ed. Tissue characterization in ultrasound, Vol. 2. Boca Raton, FL: CRC Press; 1986:169–187.

Carson, P. L.; Meyer, C. R.; Chiang, E. A.; Rubin, J. M.; Faix, R. G.; Marks, T. I. Ultrasound attenuation coefficient in fetal liver as a function of gestational age and birth. Ultrasound Med. Biol. 16(4):399–407; 1990.

Colton, T. Statistics in medicine. Boston, MA: Little, Brown and Company; 1974:136–142, 219–224.

Gluck, L.; Kulovich, M. V.; Borer, R. C.; Keidel, W. N. Interpretation and significance of the L/S ratio in amniotic fluid. American J. Obstet. Gynecol. 120(1):142–155; 1974.

Krousop, T. A.; Dougherty, D. R.; Vinson, F. S. A pulsed doppler ultrasonic system for making non-invasive measurements of mechanical properties of soft tissue. J. Rehab. Res. and Devel. 24(2):1–8; 1987.

Lerner, R. M.; Parker, K. J.; Holen, J.; Gramiak, R.; Waag, R. C. Sono-elasticity: Medical elasticity images derived from ultrasound signals in mechanically vibrated targets. Acoustical Imaging 16:317–327; 1988.

Meunier, J.; Bertrand, M.; Mailloux, G.; Petitclere, R. Assessing local myocardial deformation from speckle tracking in echography. SPIE Proc.: Medical Imaging II. 914:20–29; 1988.

Oppenheim, A. V.; Schafer, R. W. Discrete-time signal processing. Englewood Cliffs, NJ: Prentice Hall; 1989:63–67.

Papoulis, A. Probability, random variables and stochastic processes. New York: McGraw-Hill; 1965:336–352.

Thieme, G. A.; Banjavic, R. A.; Johnson, M. L.; Meyer, C. R.; Silvers, W. G.; Herron, D. S.; Carson, P. L. Sonographic indentification of fetal lung maturation. Invest. Radiol. 18:18–26; 1983.

Tristam, M.; Barbosa, D. C.; Cosgrove, D. O.; Bamber, J. C.; Hill, C. R. Application of Fourier analysis to clinical study of patterns of tissue movement. Ultrasound Med. Biol. 14(8):695–707; 1988.

Tristam, M.; Barbosa, D. C.; Cosgrove, D. O.; Nassiri, D. K.; Bamber, J. C. Ultrasound study of *in vitro* kenetic characteristics of human tissues. Ultrasound Med. Biol. 12:927–937; 1986.

Truong, X. T.; Jarrett, S. R.; Nguyen, M. C. A method for deriving viscoelastic modulus for skeletal muscle from transient pulse propagation. IEEE Trans. of Biomedical Engineering 25(4):382–384; 1978.

APPENDIX

Suppose that the time averaged relative gray-scale intensity along a given M-mode line consists of N specular reflectors distributed between epicardium and fetal chest wall. We further assume that peaks are maintained in going from systole to diastole. Let Δ_i denote the shift of the ith peak, with $i = 1$ corresponding to the epicardial reflector. If $f_i(x)$ denotes the relative gray-scale intensity of the ith peak, then

$$f_s(x) = \sum_{i=1}^{N} f_i(x)$$
$$f_d(x) = \sum_{i=1}^{N} f_i(x - \Delta_i) \tag{A1}$$

where f_s and f_d represent combined relative gray-scale distributions over the entire M-mode line in systole and diastole, respectively. Define the cross-correlation function

$$\Phi_{sd}(y) = \int f_s(x) f_d(x + y) dx, \tag{A2}$$

in which the integration is performed over the epicardial/chest wall distance and assume that cross terms may be neglected, then

$$\Phi_{sd}(y) \approx \sum_{i=1}^{N} \Phi_i(y - \Delta_i) \tag{A3a}$$

with

$$\Phi_i(y) = \int f_i(x) f_i(x + y) dx. \tag{A3b}$$

Based on empirical observation, the set $\{\Delta_i\}$ are ordered such that $\Delta_1 \geq \Delta_2 \geq \cdots \geq \Delta_N$. $\Phi_{sd}(y)$ will then display correlation peaks at $y = \{\Delta_1, \Delta_2, \ldots, \Delta_N\}$. If the width of Φ_i is sufficiently narrow, an individual peak is resolved at $y = \Delta_i$. If, on the other hand, several peaks are closely situated, a single broad peak will be apparent. Let Δ_j designate the location of the jth resolvable correlation peak consisting of N_j contributions $j = 1, 2, \ldots, N_P$, $N_P \leq N$. If Δ is the true mean deformation, then

$$\Delta \approx \sum_{j=1}^{N_P} (N_j/N) \Delta_j. \tag{A4}$$

Note that individual reflected waves vary in location along M-mode line and amplitude, but are otherwise morphologically similar. Peak amplitudes will vary due to attenuation effects, varying orientations of specular reflectors relative to the line of sight of the transducer, etc. Suppose that these amplitudes are randomly distributed and assume that the mean total power per peak Φ_0 is constant. The amplitude of the jth correlation peak will then be proportional to N_j. Let the latter be denoted by Φ_j, then

$$N_j/N \approx \Phi_j / \sum_{k=1}^{N_P} \Phi_k. \tag{A5}$$

The effect of cross-terms in eqn (A2) largely consists of peaks which occur at $y \geq \Delta_i$, although peaks whose mean separation is less than Δ_i, for some i, will contribute to the estimate of Δ. Empirically, this does not appear to be a frequent occurrence.

Let Δ_E denote the epicardial excursion, as estimated from either raw or correlation data, then the mean deformation per unit epicardial excursion is given by

$$\langle r \rangle = \Delta/\Delta_E \approx \sum_{j=1}^{N_P} \Phi_j \Delta_j / \sum_{j=1}^{N_P} \Phi_j \Delta_E. \tag{A6}$$